ISBN: 978-3-95450-132-8 doi:10.18429/JACoW-IPAC2014-TUPRI049

GEOMETRIC BEAM COUPLING IMPEDANCE OF LHC SECONDARY COLLIMATORS*

O. Frasciello†, S. Tomassini, M. Zobov, INFN-LNF, Frascati, Rome, Italy
A. Grudiev, N. Mounet, B. Salvant, CERN, Geneva, Switzerland

Abstract

The High Luminosity LHC project is aimed at increasing the LHC luminosity by an order of magnitude. One of the key ingredients to achieve the luminosity goal is the beam intensity increase. In order to keep beam instabilities under control and to avoid excessive power losses a careful design of new vacuum chamber components and an improvement of the present LHC impedance model are required. Collimators are among the major impedance contributors. Measurements with beam have revealed that the betatron coherent tune shifts were higher by about a factor of 2 with respect to the theoretical predictions based on the current model. Up to now the resistive wall impedance has been considered as the dominating impedance contribution for collimators. By carefully simulating also their geometric impedance we have contributed to the update of the LHC impedance model, reaching also a better agreement between the measured and simulated betatron tune shifts.

INTRODUCTION

The LHC collimators [1] are among the main beam coupling impedance contributors. This can be clearly seen in Fig. 1, where the detailed contributions, in percent, to the whole 2012 LHC vertical dipolar impedance model are reported [2, 3]. Here, collimators play the major role (~ 90%) over a wide frequency range, both for real and imaginary parts. At that time, in 2012, the model was essentially based on the resistive wall impedance of collimators, the resistive wall impedance of beam screens and warm vacuum pipe and a broad-band model including pumping holes, BPMs, bellows, vacuum valves and other beam instruments. The geometric impedance of collimators was approximated only by that of a round circular taper.

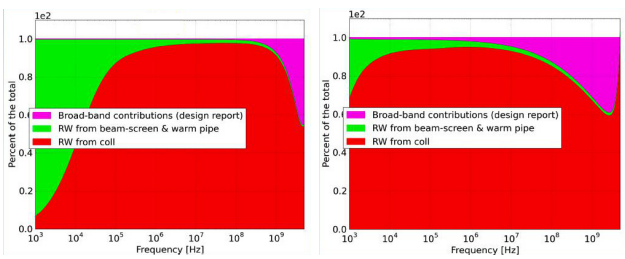

Figure 1: Real (left) and imaginary (right) parts of the 2012 LHC vertical dipolar impedance model.

* Work supported by HiLumi LHC Design Study, which is included in the High Luminosity LHC project and is partly funded by the European Commission within the Framework Programme 7 Capacities Specific Programme, Grant Agreement 284404.
† oscar.frasciello@lnf.infn.it

However, several measurements were done in 2012 of the total single bunch tune shifts vs. intensity, both at injection and at 4 TeV. A specific measurement was also performed for several collimator families all at top energy, giving their tune shifts upon moving back and forth the jaws. The experimental results, in terms of tune slope vs. intensity, were compared with the numerical simulations results, which used the wake fields from the LHC impedance model. The measured tune shifts are higher than predicted ones by a factor of ~ 2 at top energy and of ~ 3 at injection [4]; so the existing LHC impedance model accounted only for a fraction, ~ $\frac{1}{3} - \frac{1}{2}$, of the measured transverse coherent tune shifts. This fact led to the need for an LHC impedance model

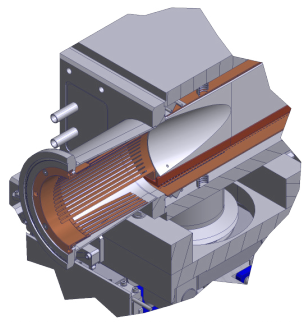

Figure 2: Detailed view of LHC collimator CAD design.

refining which, first of all, required a careful collimator geometric impedance calculation. For this purpose, we carried out numerical calculations of the geometric impedance of the LHC secondary collimator shown in Fig. 2, as close as possible to its real design and evaluated the collimator contribution to the overall LHC impedance budget.

THEORETICAL CONSIDERATIONS

In order to verify whether the geometric collimator impedance can give a noticeable contribution to the betatron tune shifts, we suggest to compare transverse kick factors due to the resistive wall impedance and the geometric one. First of all, as we show below, the tune shifts are directly proportional to the kick factors. Besides, this approach has several advantages: 1) it is a quite straightforward way to compare contributions from impedances having different frequency behaviour into the transverse tune shifts; 2) only calculations of the broad band wakes are necessary without the exact knowledge of the transverse impedance $Z_T(\omega)$; 3) both kick factors and broad band impedances are easily calculated by many numerical codes.

ISBN: 978-3-95450-132-8 doi:10.18429/JACoW-IPAC2014-TUPRI049

The well known expression for the coherent mode tune shifts can be found in [5],

$$\Delta\omega_{c_m} = j\frac{1}{1+|m|}\,\frac{I_c^2}{4\pi f_0 Q(E/e)L}\,\frac{\sum_p Z_T(\omega_p)h_m\,(\omega_p-\omega_\xi)}{\sum_p h_m\omega_p-\omega_\xi}, \tag{1}$$

where m is the azimuthal mode number, f_0 the revolution frequency, I_c is the average bunch current, Q the betatron tune, E the machine energy, L is the full bunch length and $\omega_\xi = \omega_0\frac{\xi}{\eta}$ is the "chromatic" angular frequency. For a given mode m, the bunch power spectrum for a Gaussian bunch is given by:

$$h_m(\omega) = \left(\frac{\omega\sigma_z}{c}\right)^{2|m|} e^{-\left(\frac{\omega\sigma_z}{c}\right)^2}. \tag{2}$$

Given the sum in Eq. 1 being performed over the mode spectrum lines

$$\omega_p = (p+\Delta Q)\omega_0 + m\omega_s \quad ; \quad -\infty < p < +\infty \tag{3}$$

the tune shifts are real if the imaginary transverse impedance differs from zero. For $\xi = 0$ and dipole coherent mode ($m = 0$) we get a proportionality relation:

$$\Delta\omega_{c_0} = -const\cdot I_c\sum_p \Im Z_T\,(\omega_p)e^{-\left(\frac{\omega\sigma_z}{c}\right)^2}. \tag{4}$$

On the other hand, from kick factor definition, we have

$$k_T = \frac{1}{2\pi}\int_{-\infty}^{\infty}\Im Z_T(\omega)e^{-\left(\frac{\omega\sigma_z}{c}\right)^2}\mathrm{d}\omega \tag{5}$$

so that, comparing Eq. 5 with Eq. 4, we find

$$\Delta\omega_0 \propto -k_T \tag{6}$$

In what follows we use the impedance theory developed in [2], in order to evaluate the kick factors due to the wall resistivity.

NUMERICAL CALCULATIONS

The geometric wakefields and impedances simulations were performed by means of the electromagnetic code GdfidL [6], assuming all metallic surfaces perfectly conducting.

In order to simulate the collimator as close as possible to its real design, shown in Fig. 2, we used the collimator CAD drawing including all mechanical details (.stl file) as GdfidL input file. The left picture in Fig. 3 shows the details of the collimator internal structure as presented by GdfidL, while the right picture shows the internal structure inserted into the collimator tank.

A very fine mesh (and, respectively, a huge CPU time) was necessary to reproduce in detail the long and complicated structure and to overcome numerical problems arising when simulating the long collimator tapers. In particular , we used several billions of mesh points to perform the wake fields

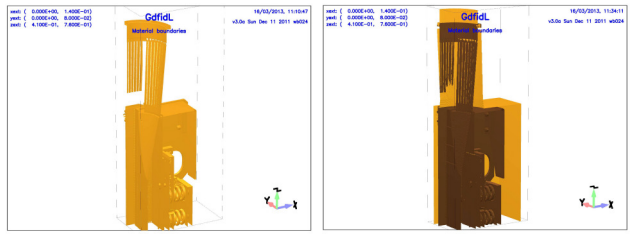

Figure 3: Collimator internal structure in GdfidL.

simulations for 2 mm long bunches that are to be used as a point-charge-like wake function in particle tracking codes.

Our numerical studies have shown that the collimator broad-band impedance is dominated by the impedance of the flat collimator tapers. In Fig. 4 (left picture) we compare the low frequency transverse impedance provided by GdfidL as a function of the collimator half gap with the analytical impedance formulas for a round taper [7] and a flat one [8], Eq. 7 and Eq. 8, respectively:

$$Z_T = j\frac{Z_0}{2\pi}\int\left(\frac{b'}{b}\right)^2\mathrm{d}z; \tag{7}$$

$$Z_T = j\frac{Z_0 w}{4}\int\frac{(g')^2}{g^3}\mathrm{d}z. \tag{8}$$

It is clearly visible that the Stupakov model (Eq. 8) is closer

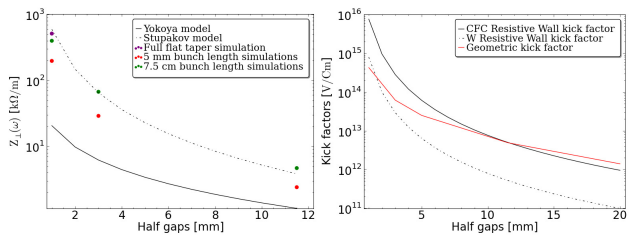

Figure 4: LHC collimator kick factors as resulting from low frequency broad-band transverse impedance GdfidL simulations (left) and kick factors comparison (right).

to simulated points than that of Yokoya (Eq. 7); there is also one point for a flat taper geometry. On the right side of Fig. 4, finally, the comparison between the geometric kick factors and the resistive wall ones, both for Carbon Fiber Composite (CFC) and Tungsten (W) made collimators' jaws, is reported, always as a function of the half gap. As a result, for W collimators geometrical impedance contribution dominates in almost the whole range of half gaps (from 1.5 mm onward), while only from about 8 mm onward for CFC collimators. Even considering the partial contribution in the case of CFC, it is evident that the geometrical impedance is not negligible with respect to resistive wall one.

Both the transverse and longitudinal impedances exhibit many resonant peaks at different frequencies. These higher order modes (HOM) are created in the collimator tank, trapped between the sliding contacts in the tapered transition etc., with parameters depending very much on the

ISBN: 978-3-95450-132-8 doi:10.18429/JACoW-IPAC2014-TUPRI049

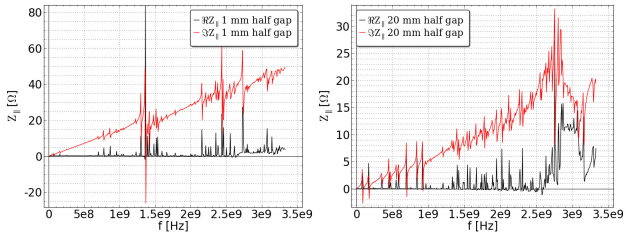

Figure 5: Real and imaginary parts of the longitudinal impedance for (left) 1 mm and (right) 20 mm half gaps.

collimator gap. As an example, Fig. 5 shows the longitudinal impedance for two different collimator gaps. We found out that the HOM parameters obtained in our simulations, such as HOM frequency patterns, their strength and dependence on the gap width are very similar to those obtained in earlier works with simpler collimator model [9–11]. The modes shunt impedances are relatively small compared to typical HOMs in RF cavities. However, possible additional RF losses and related collimator structure heating due to these modes, in the conditions of higher circulating currents in High Luminosity LHC, still deserve a deeper investigation.

Finally, in order to allow beam dynamics studies by means of particle tracking codes, detailed longitudinal and transverse dipolar and quadrupolar wake fields calculations were carried out for 5 different collimator jaws' half gaps, namely 1 mm, 3 mm, 5 mm, 11.5 mm and 20 mm. For this purpose the bunch length was just 2 mm, instead of the 7.5 cm long LHC nominal bunch length, and the wake field was traced over 1 m.

LHC IMPEDANCE MODEL UPDATE

Recently the LHC impedance model was updated taking into account several improvements, namely the evaluation of the geometric impedance of the collimators as exploited above, a full revision of the resistive wall model of the beam screens and the warm vacuum pipe, a theoretical re-evaluation of the impedance of the pumping holes, the inclusion of details of the triplet region (tapers and BPMs) and the broad-band and High Order Modes (HOMs) of the RF cavities, CMS, ALICE and LHCb experimental chambers.

Comparing the old and the updated models, a quite common impedance behaviour at low frequency and a consistent increase ($\sim 40\%$) at frequencies close to 1 GHz for the latter, can be assessed [3, 12]. This should explain a part of the factor 2 discussed in the Introduction. The impact of the geometric impedance on the whole transverse dipolar impedance LHC model is clearly visible in Fig. 6, where the various percentile contributions are shown.

CONCLUSIONS

Calculations of wake fields and beam coupling impedance have been performed for the LHC secondary collimators, for five different gaps, by means of GdfidL electromagnetic code. From the comparison of the transverse kick factors, it

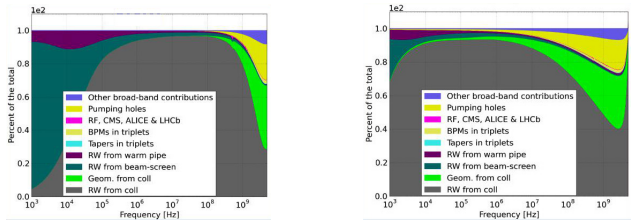

Figure 6: The updated LHC dipolar vertical impedance model real (left) and imaginary (right) parts.

has been shown that the geometric impedance contributions is not negligible with respect to the resistive wall one. In particular, for CFC made collimator, the geometrical kick starts to be comparable to resistive wall one at about 8 mm half gap. In turn, for W made collimators, the geometrical kick dominates almost for all the collimator gaps.

The present study has contributed to the refinement of the LHC impedance model. It has also been shown that the geometrical collimator impedance accounts for approximately 30% of the total LHC impedance budget, at frequencies close to 1 GHz. The work is still in progress in order to understand the origin and strengths of the HOMs trapped in the complicated collimator structure.

REFERENCES

[1] R.W. Assmann et al. An improved collimation system for the LHC. 2004.

[2] N. Mounet. *The LHC Transverse Coupled-Bunch Instability*. PhD thesis, Ecole Polytechnique, Lausanne, Mar 2012. Presented 2012.

[3] E. Metral. Initial estimate of machine impedance. (Milestone Report MS29, CERN-ACC-2014-0005), Jan 2014.

[4] N. Mounet et al. Beam stability with separated beams at 6.5 tev. In *LHC Beam Operation Workshop Evian 17-20 December 2012*, 2012.

[5] B. Zotter and F. Sacherer. Transverse instabilities of relativistic particle beams in accelerators and storage rings. *Conf.Proc.*, C761110:175–218, 1976.

[6] W. Bruns. GdfidL: A Finite Difference Program with Reduced Memory and CPU Usage. *Conf.Proc.*, C970512:2651, 1997.

[7] K. Yokoya. Resistive wall impedance of beam pipes of general cross-section. *Part.Accel.*, 41:221–248, 1993.

[8] G. Stupakov. Low Frequency Impedance of Tapered Transitions with Arbitrary Cross Sections. *Phys.Rev.ST Accel.Beams*, 10:094401, 2007.

[9] A. Grudiev. Simulation of longitudinal and transverse impedances of trapped modes in LHC secondary collimator. *CERN AB-Note-2005-042*, 2005.

[10] H. A. Day. *Measurements and Simulations of Impedance Reduction Techniques in Particle Accelerators*. PhD thesis, Manchester U., 2013. Presented 28 Jun 2013.

[11] B. Salvant. Impedance of the TCTP design. Presented at 12th TCTP design meeting, 2011.

[12] N. Mounet et al. Transverse impedance in the HL-LHC era. Presented at the 3rd Joint HiLumi LHC-LARP Annual Meeting, Daresbury, UK, 2013.